# **Evaluating QoT-Aware Hybrid Grooming Schemes in Dynamic C+L-Band Optical Networks**

Farhad Arpanaei $^{1,*,**}$ , Mohammadreza Dibaj $^{2,3,**,***}$ , Amirhossein Dibaj $^4$ , Hamzeh Beyranvand $^2$ , John S. Vardakas $^{3,5}$ , Christos Verikoukis $^6$ , José Manuel Rivas-Moscoso $^7$ , Juan Pedro Fernández-Palacios $^7$ , Alfonso Sánchez-Macián $^1$ , David Larrabeiti $^1$ , and José Alberto Hernández $^1$ 

Compiled October 8, 2025

As optical networks evolve toward dynamic, multi-band (C+L) architectures, efficient and QoT-aware resource management becomes essential to ensure scalable and low-service downtime operation. This paper introduces a novel, unified hybrid grooming framework that addresses the unique challenges of traffic grooming in dynamic multi-band elastic optical networks (MB-EONs). Motivated by the need for costeffective and adaptive high-capacity infrastructures, we propose a policy-based framework incorporating three heuristic algorithms tailored to distinct optimization goals. The unique challenges of multi-band optical networks, such as the non-uniform QoT performance caused by inter-channel stimulated Raman scattering (ISRS) are explicitly considered in our design, as they directly impact grooming efficiency, spectrum utilization, and achievable modulation formats. The algorithms include: (i) Min-Max Channel, which minimizes spectrum fragmentation and reduces partial bit rate blocking probability by up to 35%; (ii) Max Grooming Capacity, which improves line card interface (LCI) reuse and reduces deployment by 20%; and (iii) Time-Aware, which minimizes reconfiguration counts by up to 80%, significantly lowering control overhead and service downtime. Unlike prior works limited to static or single-band scenarios, our framework is the first to dynamically integrate routing, band selection, modulation format, grooming, and spectrum assignment (RBMGSA) in a QoT-aware manner. Simulation results over NSFNET, Japan, and Spain topologies under dynamic traffic conditions demonstrate that our approach supports flexible trade-offs among performance, cost, and reconfiguration complexity. Notably, the reconfigurable variants of our algorithms consistently outperform non-reconfigurable approaches by enhancing resource utilization and reducing blocking. The proposed system also supports partial grooming, enabling improved service accommodation and laying the groundwork for scalable and efficient operation in future multi-band optical networks.

© 2025 Optica Publishing Group

http://dx.doi.org/10.1364/ao.XX.XXXXXX

<sup>&</sup>lt;sup>1</sup> Department of Telematic Engineering, Universidad Carlos III de Madrid (UC3M), 28911, Leganes, Madrid, Spain.

<sup>&</sup>lt;sup>2</sup>Department of Electrical Engineering, Amirkabir University of Technology (Tehran Polytechnic), Tehran, Iran.

<sup>&</sup>lt;sup>3</sup> Iquadrat Informática, S.L., Barcelona, Spain.

<sup>&</sup>lt;sup>4</sup>Department of Electronics, Information and Bioengineering, Politecnico di Milano, P.zza Leonardo da Vinci 32, 20133 Milan, Italy.

<sup>&</sup>lt;sup>5</sup>Dept. of Informatics, University of Western Macedonia, Kastoria, Greece.

<sup>&</sup>lt;sup>6</sup>CEID, University of Patras, Greece, and ATHINA/ISI, Greece.

<sup>&</sup>lt;sup>7</sup> Telefónica Global CTIO, S/N, 28050 Madrid, Spain.

<sup>\*</sup>Corresponding author: farhad.arpanaei@uc3m.es

 $<sup>^{**}</sup>$  Farhad Arpanaei and Mohammadreza Dibaj contributed equally to this work as first authors.

<sup>\*\*\*</sup> Mohammadreza Dibaj was working in Amirkabir University of Technology, he is now with Iquadrat Informática, S.L. Supplementary material is available in [1]

### 1. INTRODUCTION

Traffic grooming in optical networks refers to the efficient aggregation of lower-rate data flows into high-capacity lightpaths to optimize the use of network resources such as transponders, amplifiers, and router/optical ports [2]. In traditional wavelengthdivision multiplexing (WDM) systems, grooming is often handled in the electrical domain, which introduces delays and increases energy consumption due to repeated optical-electricaloptical conversions [3]. With the rise of elastic optical networks (EONs), traffic grooming can be performed directly in the optical layer [4]. This optical grooming takes advantage of flexible spectrum allocation and bit rate/bandwidth-variable transponders to combine sub-wavelength traffic streams efficiently [5]. Techniques like optical tunneling and broadcast-and-select switching allow traffic from the same source to be grouped and routed without intermediate conversions or excessive guard bands [6]. This approach reduces operational costs, improves spectral efficiency, and makes the network more scalable and adaptable to dynamic traffic demands [7]. However, optical-layer grooming alone may not always be optimal [8]. For instance, if traffic flows are too small or scattered to efficiently fill an optical channel, relying solely on optical grooming may result in spectrum underutilization. This is where the hybrid approach becomes beneficial. By first aggregating small flows at the electrical layer and then grooming larger flows in the optical domain, the network can achieve better bandwidth utilization, reduce idle capacity, and lower energy consumption [7].

In dynamic environments—such as data centers or multitenant backbone networks-traffic demands can vary widely in size, duration, and routing requirements [9]. A hybrid grooming strategy offers the flexibility to adapt to these variations in realtime while maintaining a balance between performance, scalability, and energy efficiency [7]. It also allows service providers to more easily support a mix of legacy and modern services on the same infrastructure. Combining electrical-layer and opticallayer grooming leverages the strengths of both domains to address the limitations of each and achieve higher overall efficiency in optical networks. Electrical-layer grooming involves aggregating multiple low-speed client signals at routers or electrical switches before sending them to the optical layer. This method is mature and allows fine-grained control, but it requires O-E-O conversions, which are expensive in terms of power and hardware cost [10].

In a multi-band optical system—such as one that utilizes C-band, L-band, and even extended bands like S-band—the optical spectrum is divided into distinct regions, each with its own transmission characteristics in terms of attenuation, amplification requirements, and reach [11]. While this expanded spectral range significantly increases total network capacity, it also introduces new challenges in terms of resource allocation, spectrum fragmentation, equipment compatibility, and physicallayer performance [12]. Traffic grooming plays a central role in managing these complexities by intelligently aggregating and mapping multiple traffic demands across the available bands. Instead of dedicating large contiguous spectrum blocks to small or bursty flows—which leads to poor spectrum utilization and fragmentation—grooming consolidates these flows into fewer high-capacity lightpaths [13, 14], preserving spectral continuity and contiguity. Additionally, since different bands may require separate transceivers or amplifiers, grooming reduces hardware requirements by efficiently packing traffic into shared resources, lowering both capital and operational costs. Another important consideration is the varying Quality of Transmission (QoT) across bands, often measured by generalized signal-to-noise ratio (GSNR) [15]. A lightpath traversing one band may support higher-order modulation due to better QoT, while another may be limited, impacting spectral efficiency. Grooming strategies must therefore account for these QoT variations to ensure that each lightpath meets performance thresholds [16]. Furthermore, as traffic patterns become increasingly dynamic and heterogeneous, grooming must adapt in real-time to balance inter-band load, avoid congestion, and minimize the need for costly optical-electrical-optical (O-E-O) conversions [17]. Ultimately, traffic grooming in multi-band systems is not only a tool for optimizing spectral efficiency—it is an essential mechanism for enabling scalable, energy-efficient, and QoT-aware network operation in the face of ever-evolving demands [18].

In this paper, we present a comprehensive and unified framework for dynamic hybrid grooming in multi-band optical networks, addressing a critical gap in the current literature. While prior studies have focused on single-band or static scenarios, the unique challenges of grooming across multiple spectral bands—each with varying physical-layer characteristics—remain largely unexplored. Our main contributions are summarized as follows:

- We introduce three novel grooming algorithms, each targeting a distinct optimization goal in dynamic multi-band environments:
  - 1. Min-Max Channel Algorithm: Minimizes the maximum channel index used along a path to balance spectral resource utilization and reduce the partial bit rate blocking probability.
  - 2. Max Grooming Capacity Algorithm: Maximizes the reuse of spare capacity in active lightpath control instances, minimizing the need for new hardware deployments and lowering operational costs.
  - 3. Time-Aware Algorithm: Reduces network reconfiguration overhead by selecting paths that minimize changes in the current network state, thereby decreasing latency.
- We propose a unified and flexible framework that supports all three algorithms, enabling dynamic grooming decisions based on traffic patterns, physical constraints, and network policies.
- We conduct extensive performance evaluations based on key metrics including: (i) Blocking probability, to assess spectrum efficiency, (ii) Line card utilization, as a measure of hardware cost and scalability, (iii) Reconfiguration complexity, to quantify control overhead and latency.
- We demonstrate the trade-offs between efficiency, cost, and performance, showing how each algorithm can be used under different operational objectives and network conditions.

The remainder of this paper is organized as follows: Section 2 presents a comprehensive overview of the state-of-the-art techniques in hybrid traffic grooming and provides a detailed description of the current limitations. Section 3 introduces the theoretical foundations behind the proposed solution for dynamic optical networks. Section 4 presents the methodology of the proposed routing, modulation, spectrum assignment (RMSA) algorithms. Section 5 presents the simulation and analysis of

the results by incorporating graphs and tables and Section 6 concludes with a concise summary of the findings and potential directions for future research.

### 2. STATE-OF-THE-ART

The paper [3] directly focuses on grooming strategies by introducing optical-layer grooming enabled by sliceable transponders. It demonstrates how aggregating sub-wavelength traffic flows within the optical domain can significantly reduce power consumption and transponder usage. However, its scope is limited to static traffic scenarios and does not extend to dynamic or multi-band environments. The study [7] investigates dynamic resource allocation and incorporates traffic splitting and load balancing mechanisms that indirectly relate to grooming. While it improves bandwidth blocking probability, it lacks explicit grooming mechanisms that consider spectral diversity and physical-layer constraints. Similarly, the survey [19] provides a broad classification of power-saving techniques—including traffic engineering and grooming—and emphasizes their significance in energy-aware backbone networks. Nevertheless, it addresses grooming only at a conceptual level and does not delve into algorithmic design suitable for dynamic, multi-band systems.

Electrical grooming refers to the aggregation of multiple lowbit-rate client signals onto higher-capacity line card interfaces, typically within the electronic domain, to optimize resource utilization and reduce the number of optical-electrical-optical (O-E-O) conversions. Building on this concept, [20] proposes an optical-layer grooming strategy that leverages OFDM subcarrier granularity to combine multiple low-rate services into a single bandwidth-variable transponder, enhancing spectrum efficiency. In [2], a multi-layer auxiliary graph model is introduced that dynamically integrates electrical and optical-layer decisions for real-time provisioning, along with spectrum reservation techniques to support future grooming flexibility. Hardware-based solutions, such as the grooming switch with time-slot interchanging, OTDM/WDM multiplexing, and 2R regeneration presented in [21], demonstrate practical possibilities for all-optical grooming. Sliceable bandwidth-variable transponder (SBVT)-enabled grooming strategies are explored in [22], which introduces a three-layered auxiliary graph model and spectrum reservation schemes to optimize transponder utilization and reduce bandwidth blocking. Energy-efficient resource allocation using routing, traffic grooming, and transponder parameter optimization is discussed in [10], highlighting CAPEX and OPEX trade-offs. Further, [23] addresses dynamic 5G+ traffic in OTN-over-DWDM networks with a robust optimization and heuristic framework for scalable infrastructure planning. Finally, [24] demonstrates the benefits of combining traffic grooming and multi-path routing in static EONs while considering physical layer impairments, showing improved spectral efficiency and reduced resource consumption. Collectively, these works provide insights into efficient resource allocation in elastic optical networks by leveraging both electrical and optical grooming under realistic network constraints.

Collectively, these studies highlight the evolution from static, electrical and optical grooming approaches to more adaptive and flexible optical-layer grooming strategies. However, none offer a unified solution for hybrid grooming in QoT-aware dynamic multi-band networks. Our proposed framework fills this gap by enabling QoT-aware, resource-efficient, and reconfiguration-conscious grooming in future high-capacity optical systems. To

the best of our knowledge, this is the first work that systematically studies hybrid traffic grooming strategies specifically designed for multi-band optical networks in dynamic scenarios, providing a solid foundation for future developments in this emerging area.

### 3. SYSTEM DESCRIPTION

### A. Network Model

The network topology is modeled as a graph G(N,L), where N represents the set of network nodes, and L denotes the set of links connecting them. Each link utilizes a dual-fiber structure, enabling bidirectional communication through dedicated fibers for forward and backward signal transmission. The network operates within the extended C+L band, providing a total bandwidth of 12 THz, 6 THz per band. This bandwidth is further divided into 160 channels, each offering 75 GHz of spectrum, dedicated for data transmission on every fiber link.

# B. Dynamic Channel Assignment and Temporal Scheduling

A dynamic scenario is considered for the arrival of connection requests (r), each represented as  $R(s_r, d_r, \theta_r, \xi_r, \zeta_r, \tau_r)$ . Here:  $s_r$ and  $d_r$  denote the source and destination nodes of the request, randomly selected based on a uniform distribution. The data rate of each request ( $\theta_r$ ) is uniformly distributed within the range of 100 to 600 Gbit/s.  $\xi_r$  is the arrival time of the request, modeled as a random variable following a Poisson process. Consequently, the time interval between successive arrivals adheres to an exponential probability distribution with a mean inter-arrival time of  $1/\lambda$ , where  $\lambda$  is the arrival rate (requests per second).  $\zeta_r$ represents the holding time of the request, modeled as a random variable following an exponential distribution with a mean holding time of  $\mu$  seconds.  $\tau_r$  is the departure time, calculated as  $\tau_r = \xi_r + \zeta_r$ . The traffic load is measured in Erlangs and is defined as:  $\rho = \lambda \cdot \mu$ , representing the product of the arrival rate and the mean holding time. This metric reflects the ratio of the total arrival rate to the service rate. In our model, each connection request arrives randomly according to a Poisson process, and its arrival time cannot be controlled or delayed by the provisioning algorithm. At the moment of arrival, if sufficient resources are available, the request is provisioned immediately; otherwise, it is either blocked or, under the partial blocking strategy, only the portion of the request that can be accommodated is provisioned. The unmet portion is blocked and not re-scheduled at a later time. This assumption reflects a typical dynamic provisioning scenario in which blocking occurs when available resources are insufficient, without request buffering or delayed scheduling. Fig. 1 illustrates a time-domain channel allocation and scheduling scenario in a simplified elastic optical network (EON) topology consisting of three nodes (A, B, and C), interconnected by two links: A-B and B-C. Each link supports two spectral channels (Ch1 and Ch2), representing a wavelength or frequency slot. Four connection requests, denoted as R1 through R4, are established across this network over discrete time slots. Each event—i.e., the arrival or departure of a request—can only occur at a single instant, meaning that at any given time slot, either an arrival or a departure may happen, but not both simultaneously. R1 and R2 are lightpath requests originating at node A and terminating at node B, while R3 is a B-C connection. R4 is an end-to-end connection from node A to node C, which must traverse both A-B and B-C links. The temporal allocation of these requests adheres to core optical constraints, including the non-overlapping channel usage rule and the spectrum continuity

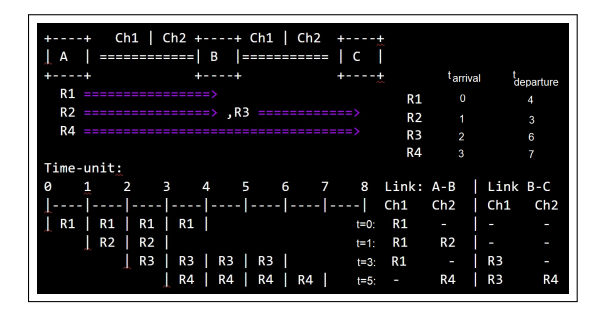


**Fig. 1.** Channel assignment and temporal scheduling of four requests (R1–R4) across a two-link, multi-channel optical network (links A–B and B–C). Each link has two channels (Ch1, Ch2), and time progresses in discrete units.

constraint—ensuring that a lightpath occupies the same channel index across all traversed links. The allocation proceeds as follows: R1 is assigned Ch1 on link A-B from time slot 0 to 4. R2 uses Ch2 on A-B between time slots 1 and 3. R3 is allocated Ch1 on B-C from time slot 2 to 6. R4 is provisioned from A to C, using Ch2 on both A-B and B-C, from time slots 3 to 7. This ensures spectrum continuity across links. Each time slot is expressed in a general time unit (TU), which could represent any duration from a second to a year. This behavior highlights the interdependence of requests in constrained networks and emphasizes the need for coordinated, physical layer impairments or QoT-aware scheduling. Indeed, in Fig. 1, while the primary focus is on the temporal and spectral allocation of connection requests, it should be noted that considering physical-layer-impairment-aware service provisioning is necessary to guarantee adequate QoT, as we show later. Physical-layer impairments, such as ASE noise, nonlinear effects, and crosstalk, can accumulate over multi-hop paths (e.g., R4 from A to C). Therefore, scheduling decisions must account not only for channel availability and spectrum continuity but also for the resulting QoT. Furthermore, the Fig. 1 underscores the challenges of dynamic provisioning in MB-EONs, where joint optimization of spectrum, time, and route is required to maintain service quality and minimize blocking.

# C. Node Architecture

In the proposed hybrid grooming framework, traffic from the client side can be aggregated onto a given LCI if the source and destination of the low-bit-rate flows are the same. As illustrated in Fig.2, the node architecture supports both electrical and optical grooming. For electrical aggregation, a fabric switch in the flex-Switchponder is used in the IP+WDM scenario, while in IP-over-WDM (IPoWDM), aggregation can occur in the router fabric. When the aggregate client traffic exceeds the maximum capacity of a single LCI, optical grooming across multiple LCIs is required. In such cases, the LCIs must share the same source, destination, and optical path to avoid jitter in the IP layer caused by latency differences across paths. This design leverages commercially deployed flex-Switchponder architectures commonly used in OTN-based backbone networks and IPoWDM scenarios. A detailed techno-economic comparison of muxponders, transponders, and OTN flex-Switchponder is beyond the scope of this work but constitutes an interesting direction for future studies.

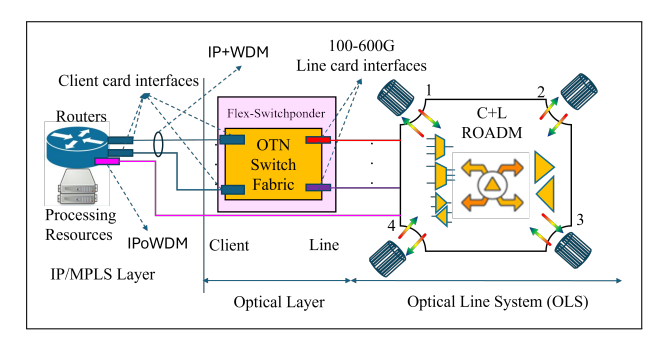


Fig. 2. Node Architecture.

#### D. QoT Estimation

For GSNR calculation, we apply an enhanced generalized Gaussian noise (EGGN) semi-closed form model to estimate the non-linear interference noise power, including the Kerr effects and inter-channel stimulated Raman Scatting (ISRS) [25, 26]. Unlike the classical GGN model, the EGGN includes an extra term that corrects for the modulation format dependence, improving the accuracy of nonlinear interference modeling. This model was validated through field trial experiments [27]. According to the concept of incoherent Gaussian Noise (GN) model for uncompensated optical transmission links [28], the end-to-end GSNR for a lightpath on channel *i* can be derived as follows:

$$\begin{split} GSNR_{LP}^{i}|_{dB} &= 10 \cdot \log_{10} \left[ \left( \Sigma_{s \in S} \kappa^{s} + \kappa_{TRx}^{-1} \right)^{-1} \right] \\ &- \kappa_{Flt}|_{dB} - \kappa_{Ag}|_{dB}, \quad \textbf{(1)} \end{split}$$

$$\kappa^{s} = (\frac{P_{\text{tx}}^{s+1,i}}{P_{\text{ASE}}^{s,i} + P_{\text{NII}}^{s,i}})^{-1}$$
 (2)

Moreover,  $P_{\rm tx}^{s+1,i}$  is the launch power at the beginning of span s+1,  $P_{\rm ASE}^{s,i}=n_{\rm F}hf^i(G^{s,i}-1)R_{\rm ch}$  is noise power caused by the Erbium-doped fiber amplifiers (EDFA) equipped with dynamic gain equalizer, and the NLI noise power ( $P_{\rm NLI}^{s,i}$ ) is calculated from (2) in [25].  $n_{\rm F}$ , h,  $f^i$ ,  $G^{s,i}=P_{\rm tx}^{s+1,i}/P_{\rm rx}^{s,i}$ , S, and  $R_{\rm ch}$  are the noise figure of EDFA (4.5 dB in the C-band and 5.5 dB in the L-band), the Planck constant, the channel frequency, the center frequency of the spectrum, the EDFA gain, the set of spans, and the channel symbol rate, respectively.  $P_{\rm rx}^{s,i}$  is the received power at the end of span s.  $\kappa_{\rm TRx}$ ,  $\kappa_{\rm Flt}$ ,  $\kappa_{\rm Ag}$  are the transceiver SNR, the SNR penalty due to wavelength selective switches filtering, and the SNR margin due to aging.

Using (1) and (2), GSNR is calculated for any lightpath from an arbitrary source to an arbitrary destination in the network. Subsequently, for each of the K shortest paths, the feasible modulation format for every channel along the path is pre-calculated by comparing the estimated GSNR of each channel to the modulation format thresholds defined in the literature [18]. Additionally, the pre-soft decision-forward error connection (FEC) bit error rate (BER) is assumed to be  $1.5 \times 10^{-2}$  [29]. The selected parameters for the bit rate, symbol rate, roll-off factor, channel spacing, and FEC overhead are 100-600 Gbps, 64 GBaud, 0.1, 75 GHz, and 20-35%, respectively. Based on equation (7) in [18], the threshold GSNR values are as follows: 3.71 dB for PM-BPSK, 6.72 dB for PM-QPSK, 10.84 dB for PM-8QAM, 13.24 dB for PM-8QAM, 16.16 dB for PM-16QAM, and 19.01 dB for

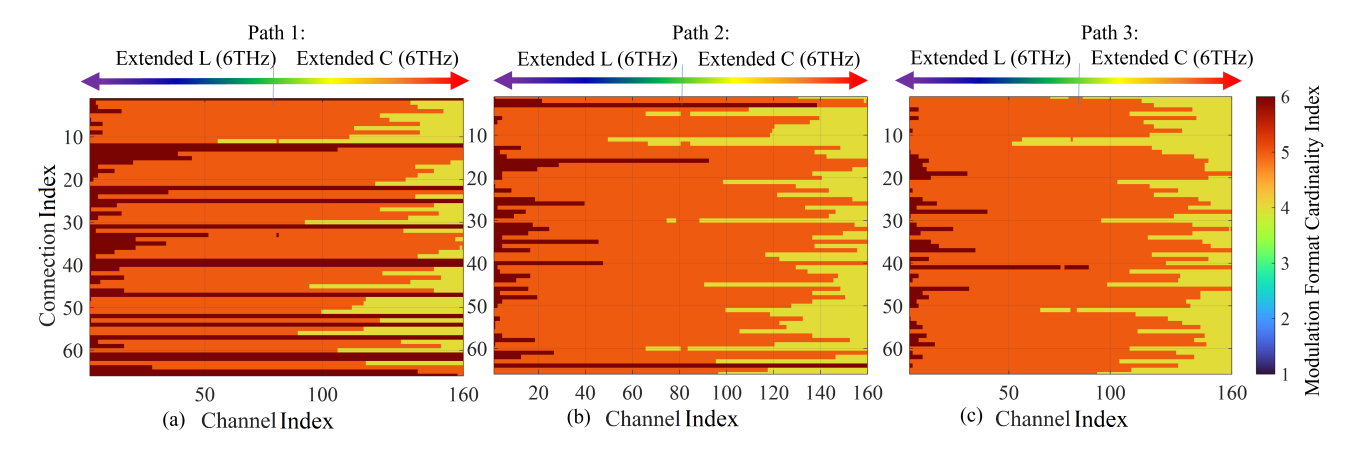


Fig. 3. Modulation format profile for k=3 shortest paths of the Japanese backbone network.

PM-64QAM with cardinality m = 2, 4, 6, 8, 10, and 12, respectively. The pre-computed modulation format levels are then used during the RBMGSA decision process to efficiently evaluate which path-channel combinations can satisfy a given bit rate request, reducing the computational overhead during service provisioning. As shown in Fig.3, an illustrative example of the Japanese backbone network is presented, with simulationbased characterizations that are explained in detail later in Section 5. The modulation format profiles for the shortest paths 1, 2, and 3 are depicted in Fig.3(a), (b), and (c), respectively. The modulation format indices range from 1, corresponding to polarization-multiplexed binary phase-shift keying (PM-BPSK) at 100 Gbps, to 6, corresponding to polarization-multiplexed 64-ary quadrature amplitude modulation (PM-64QAM) at 600 Gbps. As illustrated, the highest bitrates are observed in the long-wavelength (L)-band channels due to the ISRS effect, while the bitrates gradually decrease toward the higher-frequency end of the conventional C-band. Since each connection has a different transmission distance, the modulation formats—and thus the achievable bitrates—vary accordingly. Fig. 3 illustrates the mapping of source-destination pairs (represented by the Connection Index on the y-axis) to channel slots (represented by the Channel Index on the x-axis) across different paths. For each allocated channel, the modulation format is chosen based on the pre-computed GSNR value. As shown, channels in the L-band provide higher GSNR, enabling higher modulation format indices (e.g., 6) for shorter paths, while longer paths may require slightly lower indices (e.g., 5). Moving toward higher frequencies, ISRS reduces GSNR, which in turn lowers the achievable modulation format index (e.g., index 4 in the S-band). For instance, in the Japan topology, paths of different lengths result in the use of indices 6, 5, and 4. For brevity and to save space, the results for the Spain and US networks are not shown, but similar trends are observed. These results highlight that the distribution of modulation format indices is strongly dependent on the network size and path lengths.

# 4. QOT-AWARE DYNAMIC RESOURCE ALLOCATION AND METHODOLOGY CONCEPTS

In this section, we provide a comprehensive explanation along with the corresponding algorithm flowchart.

# A. Resource Allocation Concept

This study addresses resource allocation by focusing on the assignment of data transmission channels (transparent optical paths) between source and destination nodes, the selection of modulation formats, the allocation of line card interfaces (LCIs), and the determination of transmission paths for each request. Two critical strategies—QoT-aware traffic grooming and reconfiguration—are integrated into the allocation process to efficiently manage dynamic traffic demands.

To provide a clearer understanding of these concepts, illustrative examples are presented in Fig.4, with detailed tabular representations shown in Fig.5. Fig. 4 presents a hypothetical example to explain resource allocation. Five requests ( $r_1$  to  $r_5$ ) are sequentially allocated resources based on their source, destination, and specified paths, as depicted in the network topology. In this work, each request is assigned a modulation index (*m*) based on its estimated QoT, as described in Section D. However, in this specific example, the modulation index is assumed to be predefined for each channel to simplify the explanation. To minimize resource wastage, single-path hybrid grooming is employed. This method enables multiple requests with the same source, destination, and path to share transmission channels and LCIs, effectively improving resource utilization. For example, as illustrated in Fig. 4, request  $r_1$  has a data rate of 1100 Gbps, requiring two channels with a combined capacity of 1200 Gbps (each providing 600 Gbps). The remaining 100 Gbps of unused capacity can be allocated to other requests through traffic grooming, thereby enhancing network efficiency and minimizing resource wastage. The traffic profile—including the source, destination, path, bit rate, and the arrival and departure times of each request—is illustrated in the top-right corner of Fig. 4.

The network operations for the time intervals t=1 to 20 are depicted in Fig. 4 and further detailed in Fig. 5. In Fig. 5, the procedure of LCI deployment is illustrated at each time instant.  $N_i$  denotes an LCI deployed at node i. At the end of service provisioning, the number of  $N_i$  represents the value of LCIs at node i. We refer to this table as the LCI inventory table. As requests arrive and depart, the LCI inventory table is updated, allowing one to trace the state of LCIs in the nodes. Once all requests using a given LCI are released, that LCI becomes available to be reconfigured for a new source—destination pair or connection path. The progression of resource allocation and the dynamic changes in the network can be summarized as follows. At t=1, request  $r_1$  arrives with a data rate of 1100 Gbps. To satisfy this

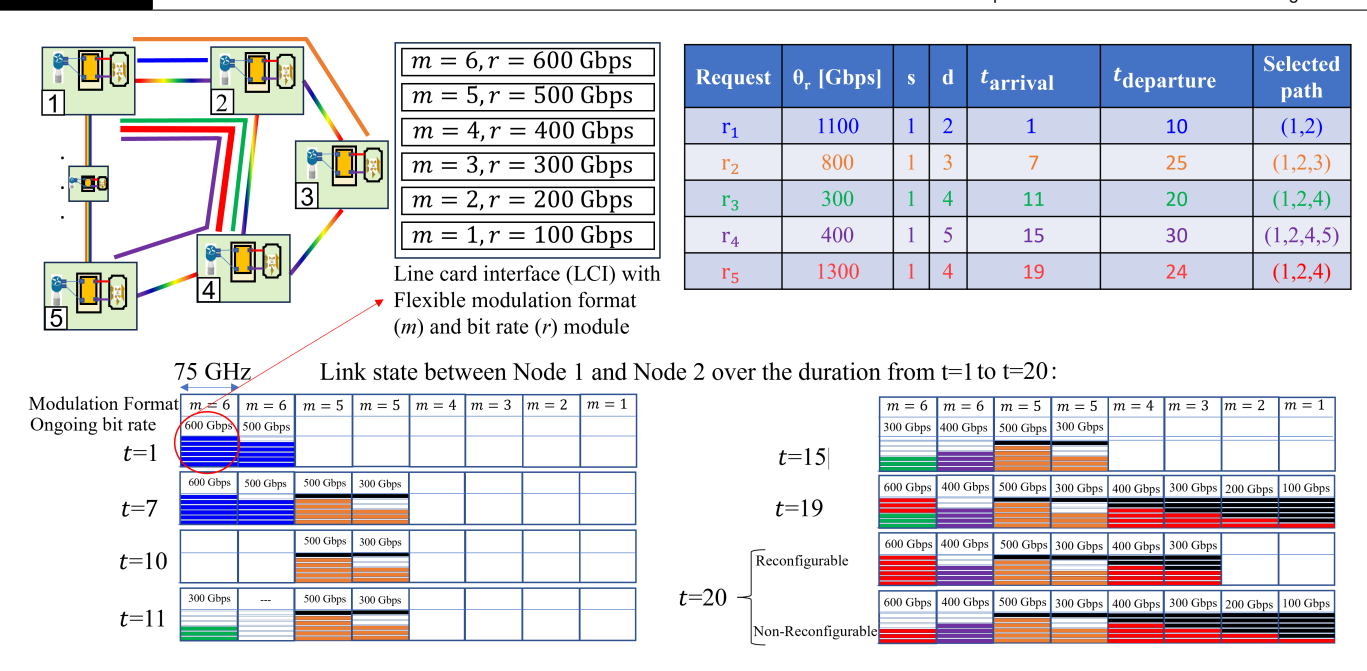


**Fig. 4.** Illustrative examples comparing reconfigurable and non-reconfigurable resource allocation scenarios. The examples demonstrate path selection, resource allocation, and traffic grooming strategies used to optimize resource utilization in dynamic optical networks.

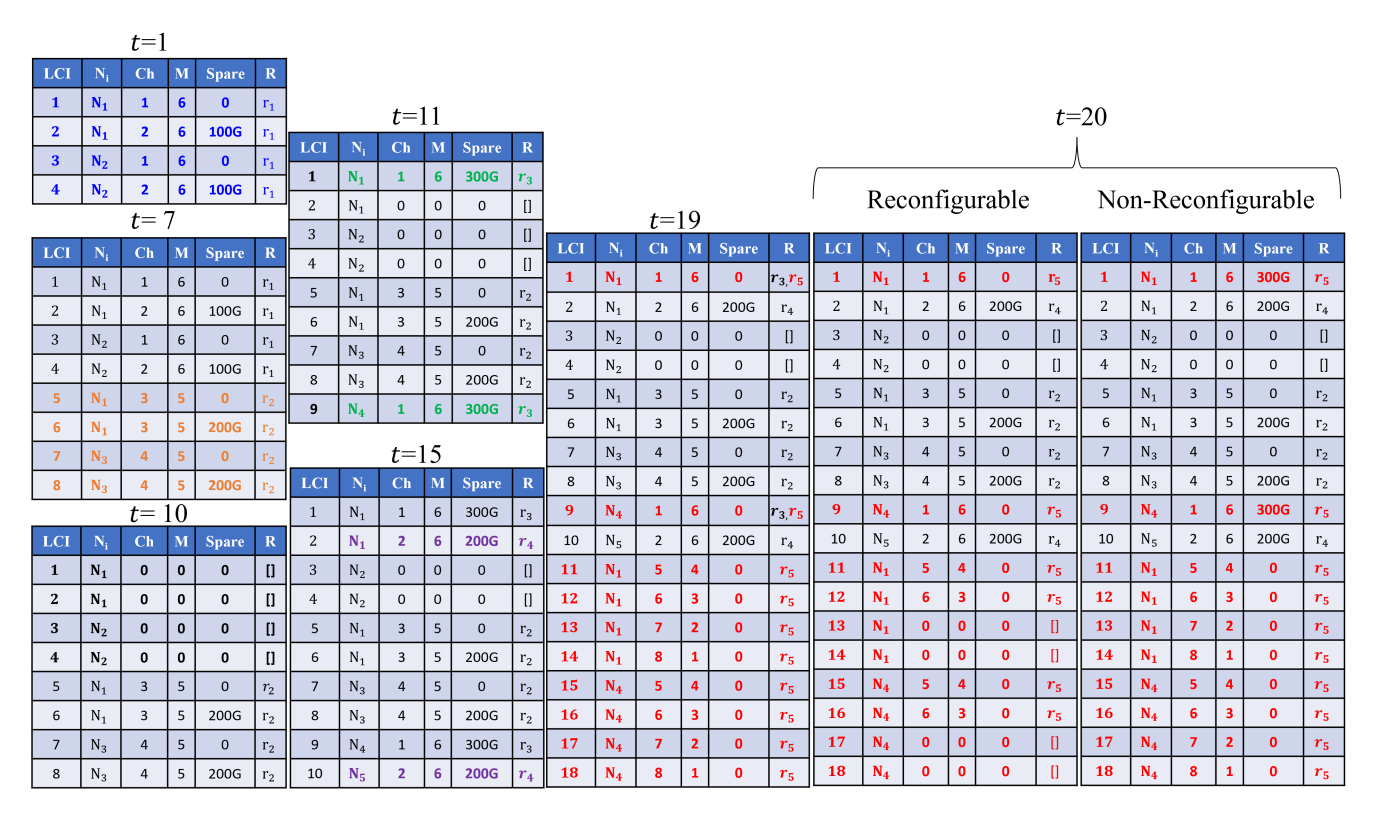


**Fig. 5.** The line card interface (LCI) inventory table representations illustrating reconfigurable and non-reconfigurable resource allocation processes. The tables highlight the state of line cards in the network, including channel usage, modulation formats, spare resources, and request assignments at different times.

request, two channels are allocated, each operating with a modulation index of m = 6, providing a total capacity of 1200 Gbps. This allocation leaves 100 Gbps of spare capacity, which remains unused at this time. At t=7, request  $r_2$  arrives with a data rate

of 800 Gbps. Similar to  $r_1$ ,  $r_2$  is allocated two channels, ensuring adequate capacity for its requirements. However, the total capacity of the allocated channels exceeds the data rate of  $r_2$ , leaving 200 Gbps of spare capacity unused. At t=10, request

 $r_1$  departs from the network, releasing channels 1 and 2, and then at t=11 request  $r_3$  arrives with a data rate of 300 Gbps.  $r_3$  is allocated one of the freed channels and uses  $LCI_1$ . However, the absence of an available LCI at the destination node necessitates the deployment of a new LCI, designated as LCI<sub>9</sub>, to accommodate the request (see Fig. 5). At t=15, request  $r_4$  arrives with a data rate of 400 Gbps. It is allocated a free LCI at the source node. However, since no spare LCI is available at the destination node, an additional LCI is deployed at the destination to support the request. At t=19, request  $r_5$  arrives with a data rate of 1300 Gbps. To optimize resource utilization, single-path grooming is applied. This technique allows 300 Gbps of  $r_5$ 's data to be transmitted using the same channel and LCIs previously utilized by  $r_3$ . By leveraging the unused capacity left by  $r_3$ , the network improves its efficiency and prevents blocking, ensuring that  $r_5$ is accommodated without requiring additional channels.

This step-by-step allocation strategy highlights the dynamic nature of the network and demonstrates how reusing and reallocating resources, such as channels and LCIs, can improve overall resource utilization and reduce network costs. At t=20,  $r_3$  departure. In a non-reconfigurable scenario, the channel used by  $r_3$  remains partially unused. However, in the reconfigurable approach, the network reallocates  $r_5$  to utilize the freed capacity, improving resource usage. This strategy reduces the maximum channel index and the number of active LCIs, as shown in Fig. 5. Specifically, the maximum channel index decreases from 8 (nonreconfigurable) to 6 (reconfigurable), and the number of active LCIs is reduced by 4, demonstrating the advantage of dynamic reconfiguration in optimizing resource allocation. Finally, it is worth noting that while dynamic reconfiguration offers numerous advantages, it also introduces additional service downtime due to the reallocation process inherent to this approach.

### **B. Methodology Concept**

To simplify the explanation of path selection and LCI allocation for each algorithm, Fig. 6 provides an illustrative example. This figure demonstrates how resources are allocated under three heuristic algorithms: Min-Max Channel, Max Grooming Capacity, and *Time-Aware*. At t = 5, with requests  $r_1$  to  $r_4$  already allocated, the algorithms evaluate the current network state to select the optimal path based on their specific criteria. The Min-Max Channel Algorithm minimizes the maximum channel index by selecting the path with the lowest channel index among all candidate paths. As shown in Fig. 6, path (1,3,4) is selected because it achieves the lowest maximum channel index, effectively balancing resource utilization across the network. The Max Grooming Capacity Algorithm prioritizes maximizing the spare capacity of active LCIs along each candidate path. This approach reduces the need for deploying new LCIs, thereby lowering network costs. According to Fig. 6, path (1,4) is selected, as it leverages the available spare capacity of existing LCIs while avoiding the need for additional deployments. The Time-Aware Algorithm focuses on minimizing reconfiguration counts to reduce network latency. As illustrated in Fig. 6, path (1, 2, 4) is chosen because it requires no reconfiguration, ensuring the lowest possible delay during dynamic adjustments. This example, as depicted in Fig. 6, highlights how each algorithm optimizes a specific aspect of resource allocation: balancing channel utilization, minimizing LCI deployment costs, and reducing reconfiguration-induced latency. These approaches demonstrate the trade-offs between efficiency, cost, and performance in dynamic optical networks. At t = 5, with requests  $r_1$  to  $r_4$  already allocated, the algorithms evaluate the current network state to select the optimal path for

the new request  $r_5$ . The Min-Max Channel Algorithm minimizes the maximum channel index by selecting the path with the lowest channel index among all candidate paths. As shown in Fig. 6, path (1, 3, 4) is selected because it achieves the lowest maximum channel index, thereby balancing resource utilization across the network. In this approach, since the departure time of  $r_4$  occurs before that of  $r_5$ , the algorithm triggers a reconfiguration upon  $r_4$ 's release. As a result, the entire 300 G of  $r_5$  is accommodated on channel 1 of the path state. It should be noted that the path state is obtained by applying a logical OR operator on the states of the links along the path, where an occupied channel is represented as 1 and an idle channel as 0. As shown in Fig. 6, the maximum utilized channel index for this algorithm is lower than that of the others. The Max Grooming Capacity Algorithm aims to minimize the spare capacity of active LCIs along each candidate path. This reduces the need for deploying new LCIs and therefore lowers network costs. According to Fig. 6, path (1,4) is selected, as it leverages the available spare capacity of existing LCIs while avoiding additional deployments. In this case, a reconfiguration occurs when  $r_1$  departs earlier than  $r_5$ , allowing  $r_5$  to migrate to channel 1. As illustrated in Fig. 6, the LCI usage of this algorithm is lower than that of the others. The *Time-Aware Algorithm* focuses on minimizing the number of reconfigurations to reduce service downtime. As shown in Fig. 6, path (1,2,4) is selected because it requires no reconfiguration: the departure times of  $r_2$  and  $r_3$  occur later than that of  $r_5$ . Since departure times are explicitly considered to minimize reconfiguration, this approach is referred to as time-aware. As highlighted in Fig. 6, the reconfiguration count of this algorithm is lower than that of the others. This example illustrates how each algorithm optimizes a distinct aspect of resource allocation: balancing channel utilization, minimizing LCI deployment costs, or reducing reconfiguration-induced downtime. Together, these approaches highlight the trade-offs between efficiency, cost, and performance in dynamic optical networks. The implementation of these algorithms is publicly available at [1].

### C. The proposed RBMGSA algorithms

A heuristic algorithm is proposed to provide a near-optimal solution for the QoT-Aware Routing, Band, Modulation Format, Grooming, and Spectrum Assignment (RBMGSA) problem in large-scale dynamic optical networks. The flowchart of the proposed algorithm is presented in Fig. 7, outlining the steps for path selection, modulation format selection, spectrum assignment, and LCI assignment. The algorithm incorporates three resource allocation methods: Min-Max Channel, Max Grooming Capacity, and Time-Aware, each of which can operate under two approaches: non-reconfigurable, where no reallocation of resources occurs after the initial assignment, and reconfigurable, where dynamic reallocation is allowed to optimize performance.

Additionally, we employ a *partial bit rate blocking probability* strategy for resource allocation. In cases where the available resources are insufficient to fully meet a request, the algorithm allocates the available portion and blocks only the remaining unmet demand. For example, if a request requires a data rate of 400 Gbps but only 200 Gbps are available, the algorithm assigns 200 Gbps and blocks the rest. This strategy is more efficient than traditional methods, which block the entire request in such scenarios. By enabling partial bit rate blocking probability, it improves resource utilization and reduces the overall blocking probability.

The algorithm begins with the initialization of the network topology and traffic characteristics, as described in Sections 3.A

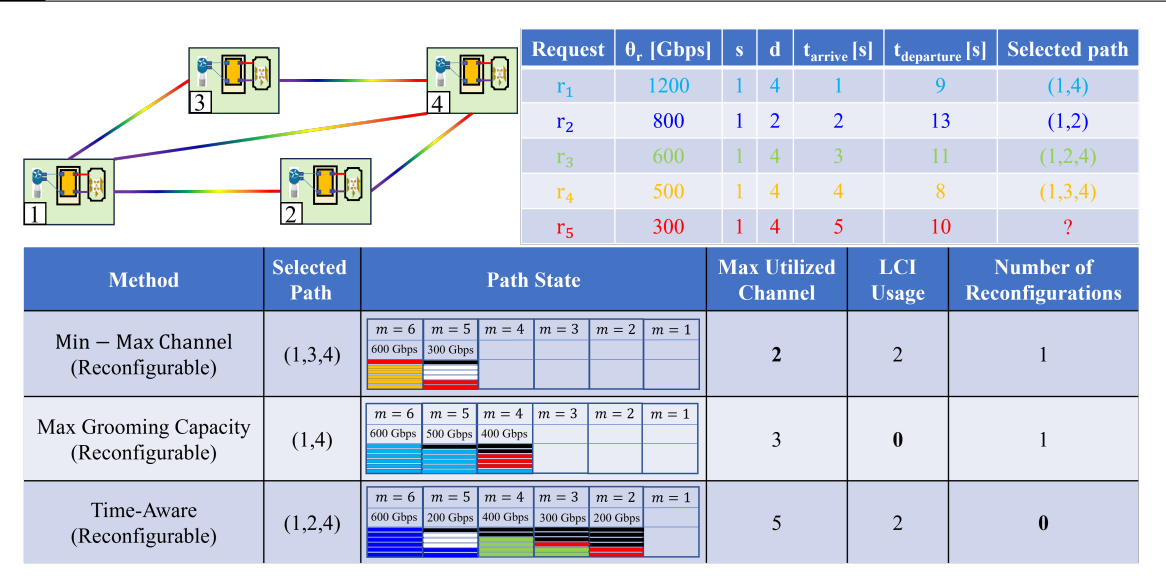


**Fig. 6.** Illustrative examples of resource allocation in the Min-Max Channel, Max Grooming Capacity, and Time-Aware (Reconfigurable) methods, showing path selection, path state, maximum channel utilization, line card usage, and reconfiguration counts, providing a comparative analysis of each method.

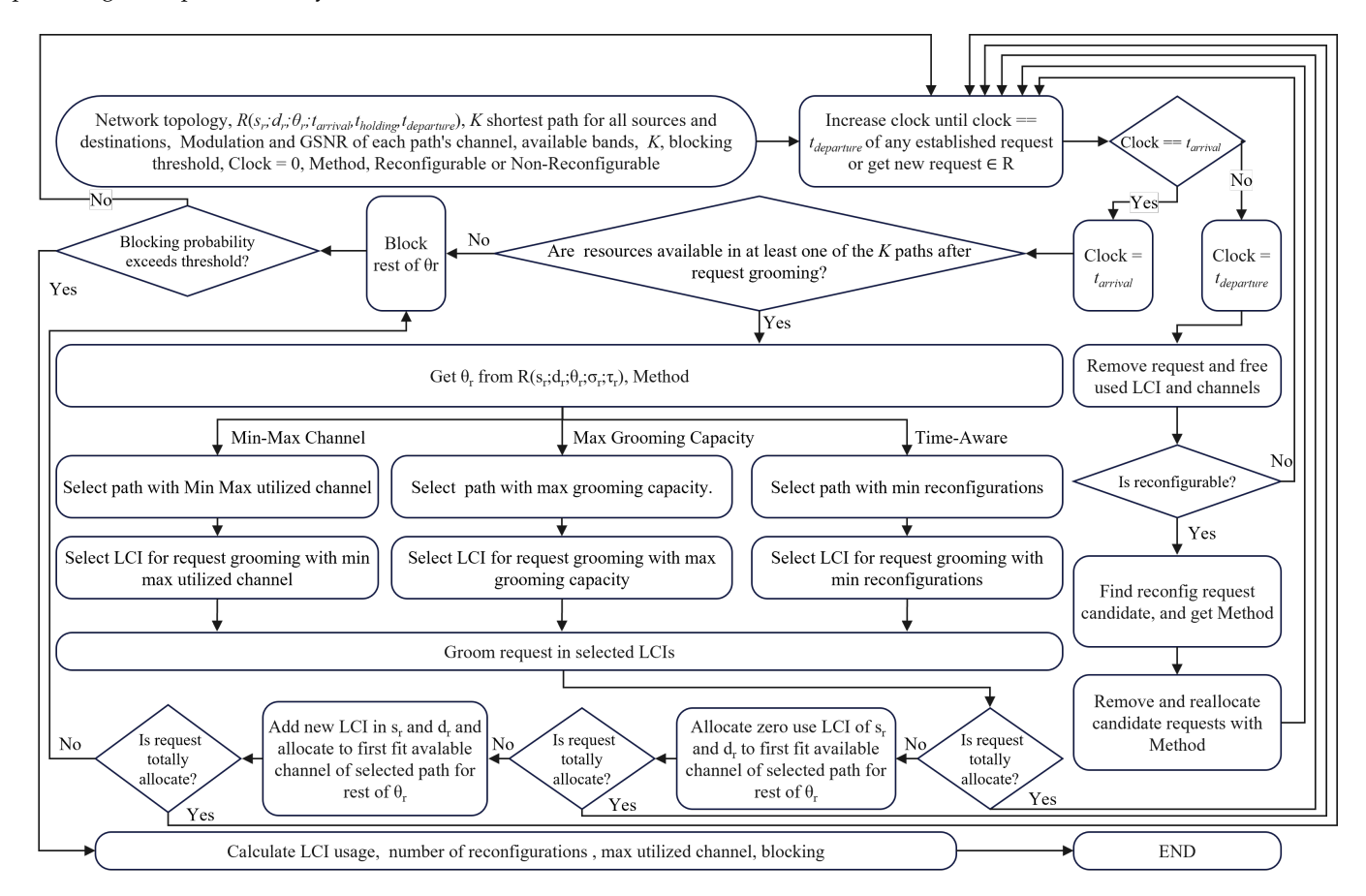


**Fig. 7.** Flowchart of the heuristic algorithm, which incorporates three resource allocation methods—Min—Max Channel, Max Grooming Capacity, and Time-Aware. Each method operates under two approaches: non-reconfigurable and reconfigurable. The flowchart illustrates their processes for routing, band, modulation format selection, grooming, and spectrum assignment (RB-MGSA) in dynamic optical networks.

and 3.B. The network utilizes a dual-fiber structure within the extended C+L band, supporting dynamic traffic requests.For each incoming request, *K* candidate paths are computed based

on pre-determined shortest paths using Yen's k-shortest-path method. These paths are then evaluated for resource allocation suitability as described in Section 3.B. Once the candidate paths

are established, the modulation format is selected for each path based on the estimated QoT as described in Section 3.D.

After the modulation format is determined, the algorithm performs spectrum assignment. This involves checking the availability of contiguous channels along each candidate path and applying a first-fit allocation strategy to assign the required channels. The resource allocation method is then applied to select the most suitable path. The Min-Max Channel method minimizes the maximum channel index to reduce fragmentation, while the Max Grooming Capacity method prioritizes paths with the highest spare capacity along active LCIs, minimizing the need for new LCI deployments. The Time-Aware method reduces latency by selecting paths that require the fewest reconfigurations. Once the optimal path is selected, the LCI assignment process is carried out. If the selected path lacks an active LCI with sufficient capacity, a new LCI is deployed along the path. In cases where active LCIs can accommodate the request, the existing resources are utilized instead. For algorithms operating under the reconfigurable approach, the network may dynamically reallocate resources to further optimize performance and reduce fragmentation. In contrast, the non-reconfigurable approach skips this reallocation step.

It is worth noting that while we did not explicitly evaluate spectrum fragmentation in this study, the use of the Min-Max Channel algorithm inherently mitigates fragmentation (see Fig. 6). This approach prioritizes packing active channels toward the lower indices of the frequency spectrum, which increases spectral efficiency and intuitively reduces fragmentation. Although fragmentation metrics are not reported here, the correlation between minimizing the maximum utilized channel and reducing fragmentation has been demonstrated in our prior works [14, 30, 31], where it was shown that this strategy leads to more contiguous spectrum usage and, consequently, lower blocking probability.

Finally, the selected path, modulation format, spectrum assignment, and LCI allocation are finalized. The network state is updated to reflect the new allocation, and the algorithm proceeds with the next request. By combining the three resource allocation methods and incorporating both reconfigurable and non-reconfigurable approaches, along with a *partial bit rate blocking* strategy, the proposed RBMGSA algorithm offers an efficient and flexible solution to address the challenges of resource management in dynamic optical networks.

### 5. SIMULATIONS AND NUMERICAL RESULTS

In this section, we evaluate the performance of the proposed RBMGSA algorithms under varying traffic loads across three representative network topologies: NSFNET, JP, and SP (Fig. 8). To ensure statistical reliability, each simulation was executed multiple times until a 95% confidence level was achieved, and the results presented are based on average values. To ensure the statistical reliability of our simulation results, in each simulation run we generated 100,000 connection requests. Each experiment was repeated multiple times until the half-width of the 95% confidence interval for the measured performance metrics—such as blocking probability, maximum channel utilization, LCI usage, and reconfiguration counts—was below 5% of the corresponding sample mean. To do so, Each simulation was executed 100 independent times, and the reported results include 95% confidence intervals calculated using the standard error of the mean from CI<sub>95%</sub> =  $\bar{X} \pm 1.96 \cdot \frac{\sigma}{\sqrt{n}}$ , where  $\bar{X}$  is the sample mean,  $\sigma$  is the sample standard deviation, and n is the number of runs [32].

Error bars are not shown in the figures to avoid visual clutter, but the confidence intervals were carefully monitored to ensure they are narrow (typically less than 5% of the mean), confirming that the results are statistically reliable. The evaluation focuses on key performance metrics, including maximum utilized channels, partial bit rate blocking probability, LCI usage, and reconfiguration counts. These metrics provide critical insights into the trade-offs among resource efficiency, operational costs, and latency across the three heuristic algorithms—Min-Max Channel, Max Grooming Capacity, and Time-Aware—operating under both reconfigurable and non-reconfigurable approaches.

In our work, we define the *partial bit rate blocking probability* as the fraction of a request's bit rate that cannot be established (see Eq. (3)). In other words, when only part of the requested bit rate can be provisioned, we report the unestablished portion as blocked. This approach aligns with real-world scenarios, where telecom operators typically allow customers to establish as much of the requested traffic as possible in dynamic environments, and the service level agreement is defined based on the established portion of the traffic. This strategy differs from a strict all-ornothing blocking approach, in which a request is either fully established or fully blocked. For simplicity, throughout the remainder of the paper, we refer to this metric as the *blocking*, although it actually corresponds to the partial bit rate blocking probability.

$$B_{\text{partial}} = \frac{\sum_{i=1}^{N} \left( R_i^{\text{requested}} - R_i^{\text{established}} \right)}{\sum_{i=1}^{N} R_i^{\text{requested}}}$$
(3)

where  $B_{\mathrm{partial}}$  is the partial bit rate blocking probability. N is the total number of requests.  $R_i^{\mathrm{requested}}$  is the bit rate requested by the i-th request.  $R_i^{\mathrm{established}}$  is the bit rate actually established for the i-th request.

Fig. 9 illustrates the relationship between maximum channel utilization and offered traffic load for the NSFNET, JP, and SP topologies. The results highlight the superior performance of the Min-Max Channel algorithm, particularly when using the reconfigurable approach, in minimizing channel utilization. For instance, in the NSFNET topology at an offered traffic load of 500 Erlangs, the Min-Max Channel algorithm under the reconfigurable approach achieves a maximum utilized channel of 63, compared to 70 in the non-reconfigurable configuration. Conversely, the Max Grooming Capacity algorithm, which prioritizes leveraging spare capacity in active channels, shows higher maximum channel utilization with values of 99 and 106 for the reconfigurable and non-reconfigurable configurations, respectively. The Time-Aware algorithm exhibits the highest channel utilization, with a value of 150 in the reconfigurable configuration. In the JP topology at an offered traffic load of 600 Erlangs, the Min-Max Channel algorithm reduces the maximum utilized channel to 101 under the reconfigurable approach, outperforming the Max Grooming Capacity and Time-Aware algorithms, which achieve maximum utilized channel values of 133 and 156, respectively. Similarly, in the SP topology at an offered traffic load of 1100 Erlangs, the Min-Max Channel algorithm under the reconfigurable approach provides the best performance, with a maximum channel index of 100, compared to 136 for Max Grooming Capacity and 151 for Time-Aware. These results emphasize the effectiveness of the Min-Max Channel algorithm in decreasing blocking probability by prioritizing paths with the lowest channel indices. As discussed in Section 4, the reconfigurable approach further improves resource allocation by

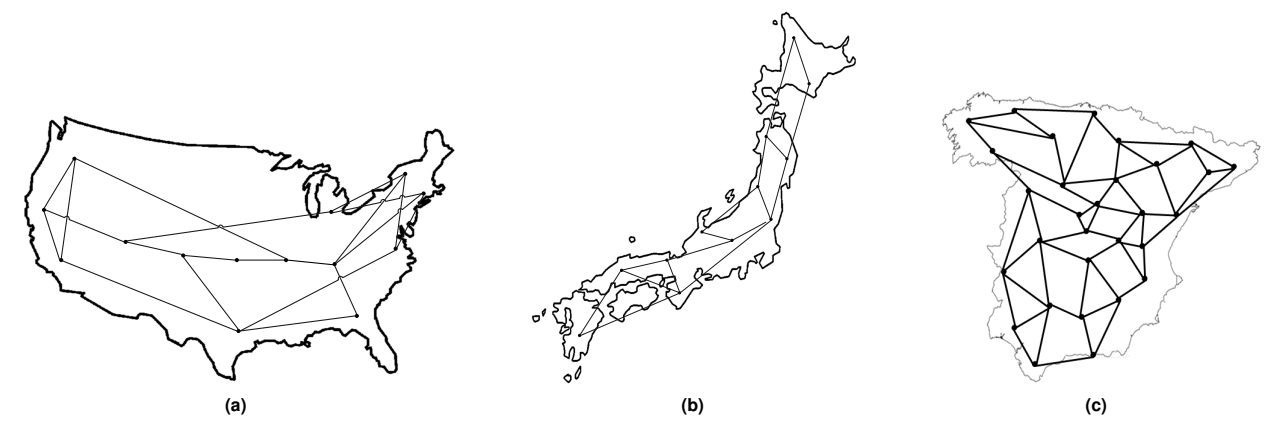


**Fig. 8.** The considered network topologies: (a) National Science Foundation Network (NSFNET) with 14 nodes and 22 links, (b) Japanese Backbone Network (JP) with 12 nodes and 17 links, and (c) Spanish Backbone Network (SP) with 30 nodes and 55 links.

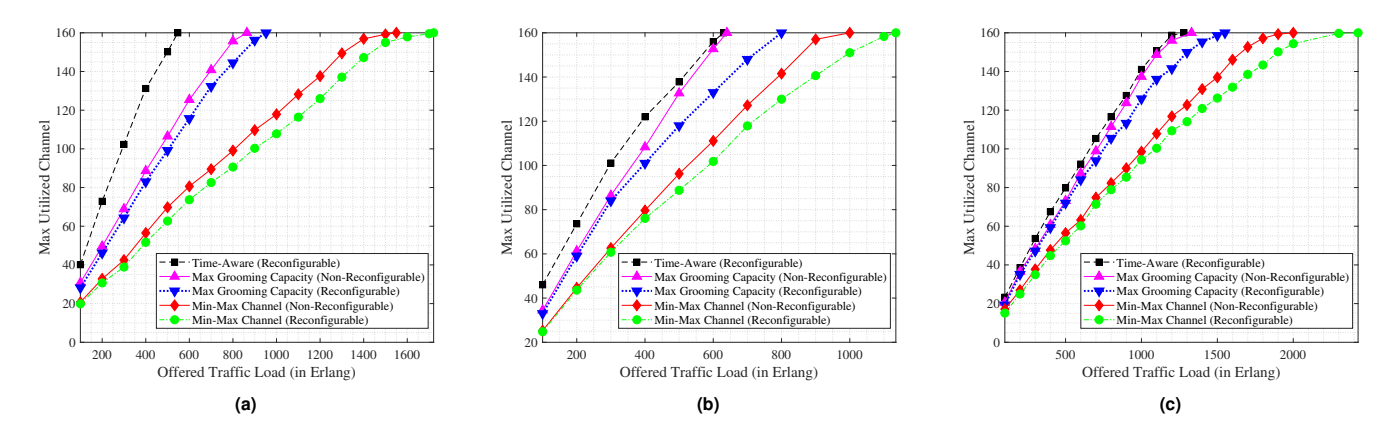


Fig. 9. Max Utilized Channel versus Offered Traffic Load (in Erlang) for (a) NSFNET, (b) JP, and (c) SP for 1% blocking threshold.

dynamically reallocating freed capacities, thereby reducing the maximum utilized channel and decrease the blocking probability mitigating fragmentation across the network.

The blocking results, presented in Fig. 10, reinforce the trends observed in Fig. 9. In the NSFNET topology, at a blocking threshold of 1%, the Min-Max Channel algorithm supports up to 1721 Erlangs under the reconfigurable approach, significantly outperforming its non-reconfigurable counterpart, which supports 1550 Erlangs. In comparison, the Max Grooming Capacity algorithm accommodates up to 952 Erlangs in the reconfigurable configuration, compared to 864 Erlangs in the non-reconfigurable setting. The Time-Aware algorithm demonstrates the highest blocking among the three, supporting only 547 Erlangs in its reconfigurable configuration. These results emphasize the superior performance of the Min-Max Channel algorithm in managing higher traffic loads, especially when employing dynamic reconfiguration. In the JP topology, the Min-Max Channel algorithm again shows superior performance, accommodating 1135 Erlangs in the reconfigurable configuration compared to 1000 Erlangs in the non-reconfigurable configuration. The Max Grooming Capacity algorithm achieves lower thresholds, supporting 800 Erlangs with reconfiguration and 640 Erlangs without it. A similar trend is observed in the SP topology, where the Min-Max Channel algorithm supports up to 2427 Erlangs under the reconfigurable approach, significantly surpassing the 2000

Erlangs supported by the non-reconfigurable approach. These findings highlight the advantage of the reconfigurable approach in reducing blocking through dynamic resource reallocation, as elaborated in Section 3.B.

Fig. 11 illustrates the trends in LCI usage across the three network topologies. The Max Grooming Capacity algorithm consistently demonstrates the lowest LCI usage, highlighting its efficiency in consolidating traffic into existing LCIs and minimizing new deployments. For example, in the SP topology at a traffic load of 1100 Erlangs, the reconfigurable Max Grooming Capacity algorithm utilizes 1222 LCIs, compared to 1307 LCIs in the non-reconfigurable configuration. The Min-Max Channel algorithm shows slightly higher LCI usage under the same conditions, with 1311 LCIs in the reconfigurable case and 1380 LCIs in the non-reconfigurable configuration. In contrast, the Time-Aware algorithm records the highest LCI usage, reaching 1453 LCIs in the reconfigurable approach, as it prioritizes minimizing reconfiguration latency over resource efficiency. In the NSFNET topology at a traffic load of 500 Erlangs, the reconfigurable Max Grooming Capacity algorithm reduces LCI usage to 790 LCIs, compared to 830 LCIs for the non-reconfigurable configuration. The Min-Max Channel algorithm records 871 LCIs in the reconfigurable case, balancing channel utilization and grooming efficiency. These results emphasize that, among the considered algorithms, the Max Grooming Capacity algorithm achieves the

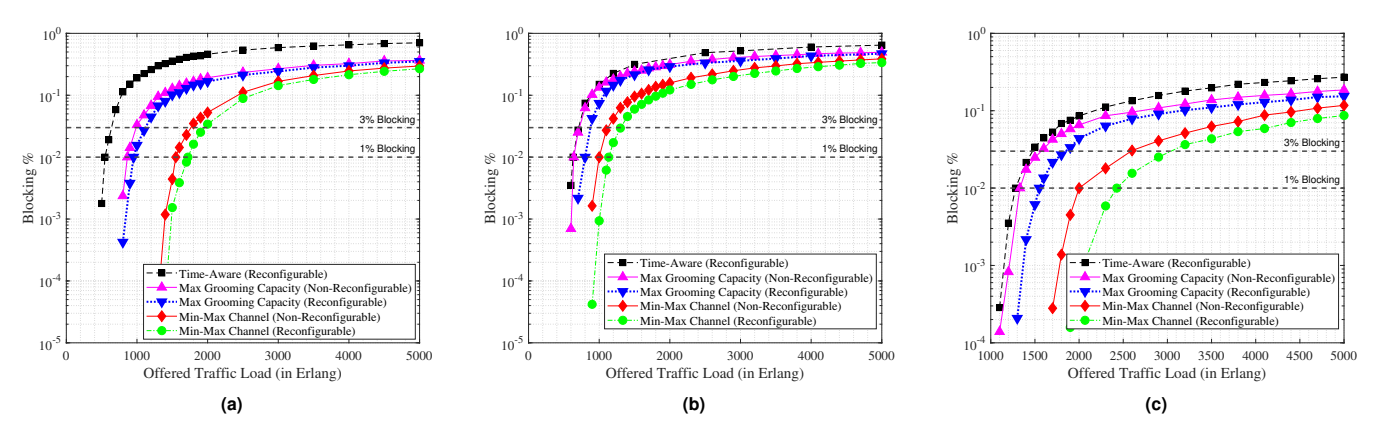


Fig. 10. Blocking versus Offered Traffic Load (in Erlang) for (a) NSFNET, (b) JP, and (c) SP.

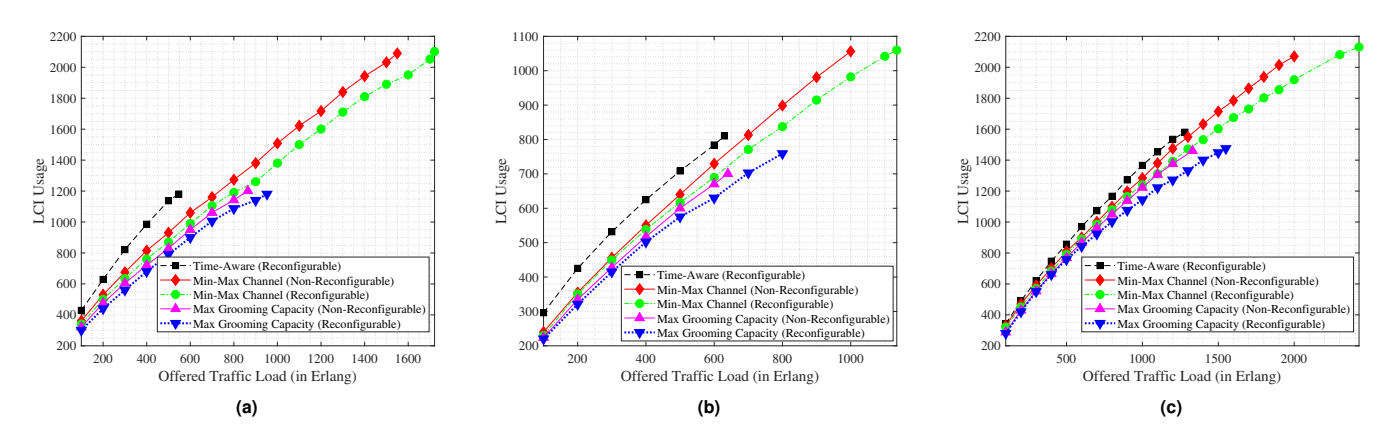


Fig. 11. Line Card Interface (LCI) Usage versus Offered Traffic Load (in Erlang) for (a) NSFNET, (b) JP, and (c) SP for 1% blocking threshold.

lowest LCI usage, while the reconfigurable Min-Max Channel algorithm offers a balanced trade-off by effectively reducing blocking while maintaining efficient LCI deployment.

Reconfiguration counts, shown in Fig. 12, underscore the trade-offs between minimizing reconfigurations and optimizing resource allocation. Among the evaluated algorithms, the Time-Aware algorithm achieves the lowest reconfiguration counts across all topologies. In the NSFNET topology at an offered traffic load of 500 Erlangs, the Time-Aware algorithm records just 2095 reconfigurations, significantly fewer than the 8956 reconfigurations required by the Min-Max Channel algorithm and the 11,036 reconfigurations incurred by the Max Grooming Capacity algorithm under the same conditions. Similarly, in the IP topology at an offered traffic load of 600 Erlangs, the Time-Aware algorithm performs exceptionally well, requiring only 6227 reconfigurations. In contrast, the Min-Max Channel and Max Grooming Capacity algorithms necessitate 13,657 and 15,360 reconfigurations, respectively. These results highlight the ability of the Time-Aware algorithm to reduce latency by minimizing reconfiguration events. However, this advantage comes at the cost of increased LCI usage and blocking as illustrated in Figs. 10 and 11.

In the SP topology, the Time-Aware algorithm also demonstrates the lowest reconfiguration counts, with values of 3000, compared to 9200 and 10,200 for the Min-Max Channel and Max

Grooming Capacity algorithms, respectively. These findings emphasize the capability of the Time-Aware algorithm to minimize reconfiguration events, thereby reducing network service downtime and operational overhead. However, this advantage comes at the expense of higher blocking probabilities and increased LCI usage, as observed in earlier results (Figs. 10 and 11). The results underscore the inherent trade-offs among the three heuristic algorithms, underscoring the importance of selecting an approach based on the specific requirements of dynamic optical networks. The Min-Max Channel algorithm excels in minimizing maximum channel utilization, making it ideal for scenarios that prioritize spectral efficiency. Conversely, the Max Grooming Capacity algorithm effectively reduces LCI deployment costs, demonstrating its suitability for cost-sensitive applications. Meanwhile, the Time-Aware algorithm minimizes reconfiguration counts, thereby reducing service downtime; however, this benefit comes at the expense of higher blocking and increased resource usage. These observations align with the conceptual analyses outlined in Section 4, further validating the practical effectiveness of the proposed algorithms in dynamic optical networks. Notably, reconfigurable approaches consistently outperform their nonreconfigurable counterparts in terms of resource efficiency and adaptability. However, this improvement comes with a minor trade-off in reconfiguration-induced service downtime, which should be carefully considered based on network design priori-

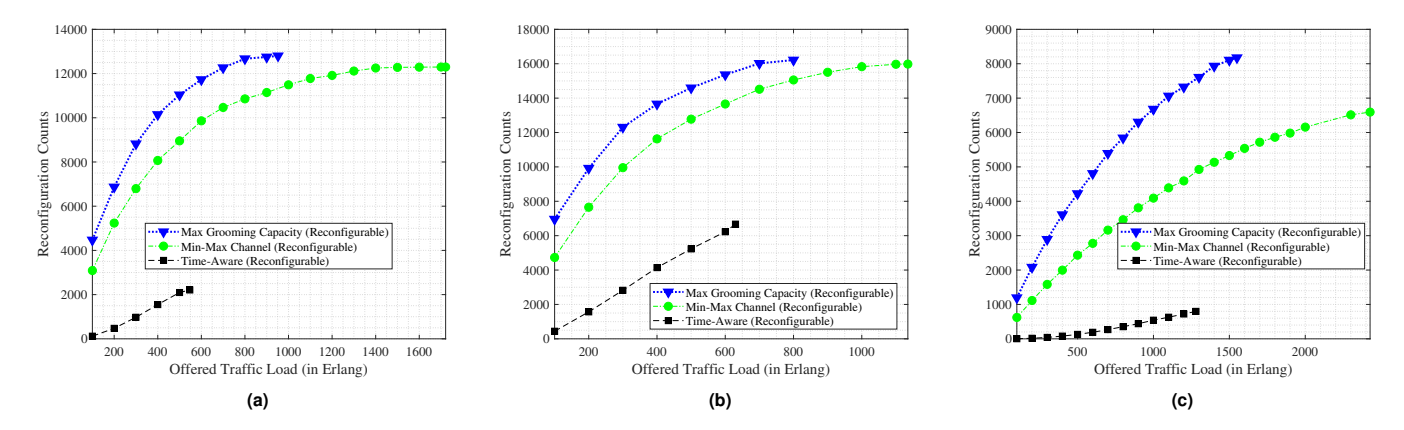


Fig. 12. Reconfiguration Counts versus Offered Traffic Load (in Erlang) for (a) NSFNET, (b) JP, and (c) SP for 1% blocking threshold.

ties.

We note that reconfiguration results in temporary service downtime or brief interruptions. In the C+L-band systems considered in this work, ASE noise loading is used to fill idle channels, keeping the network link states unchanged. As a result, reconfiguration primarily involves minor adjustments of line card frequencies and ROADM settings. Furthermore, the optimal reconfiguration scenario can be precomputed in a digital twin, as proposed in [33], and applied to the network with minimal disruption.

### 6. CONCLUSION

This study presents a comprehensive and dynamic hybrid grooming framework for C+L-band optical networks, addressing the critical challenge of efficiently managing heterogeneous traffic demands in multi-band environments. By integrating three complementary heuristic algorithms-Min-Max Channel, Max Grooming Capacity, and Time-Aware-into a QoTaware resource allocation framework, the proposed solution enables flexible optimization according to different network objectives, including spectral efficiency, cost-effectiveness, and service downtime minimization. Extensive simulations over diverse topologies (NSFNET, JP, and SP) confirm that: (i) The Min-Max Channel algorithm excels at decreasing the blocking probability by reducing the maximum channel index, thereby supporting higher traffic loads with lower blocking probabilities. (ii) The Max Grooming Capacity algorithm is particularly effective in minimizing line card interface (LCI) usage by reusing existing capacity, making it ideal for cost-sensitive deployments. (iii) The Time-Aware algorithm significantly reduces the number of reconfiguration events, thus lowering control overhead and service latency—an important benefit in latency-critical services like 5G/6G or cloud interconnects. Importantly, the reconfigurable versions of all three algorithms consistently outperform their non-reconfigurable counterparts by dynamically reallocating freed resources, achieving better spectrum utilization and reduced blocking. The integration of partial bit rate blocking further enhances the efficiency of the system by serving partial demand when full provisioning is not possible. The integration of partial blocking is expected to further enhance system efficiency by serving partial demand when full provisioning is not possible, although this effect is not explicitly evaluated in the present study.

Overall, this work demonstrates that the proposed RBMGSA framework can support different performance objectives by selecting the appropriate heuristic, providing a flexible foundation for scalable, cost-efficient, and high-performance operation in multi-band optical networks. Future work may explore adaptive balancing of competing metrics, integration of machine learning for predictive grooming, and extension to S-band or ultra-wideband transmissions.

# **FUNDING AND ACKNOWLEDGMENTS**

Authors from UC3M would like to acknowledge the support of the EU-funded 6G SNS SEASON project (grant No.101096120) and EU-funded FLEX-SCALE project (grant No.101096909), and the Spanish-funded Fun4date-Redes project (grant No.PID2022-136684OB-C21), and TUCAN6-CM project (Grant No. TEC-2024/COM-460) funded by the Community of Madrid (ORDER 5696/2024). Finally, authors from Iquadrat Informática and University of Patras would like to acknowledge the support of the EU-funded 6G SNS project ADROIT-6G (grant No. 101095363).

# **REFERENCES**

- F. Arpanaei, "Implementation of QoT-aware hybrid grooming schemes in dynamic C+L-band optical networks: Source codes and datasets," Zenodo, Software / Data repository (2025). Available: https://doi.org/ 10.5281/zenodo.17287687.
- S. Zhang, C. Martel, and B. Mukherjee, "Dynamic traffic grooming in elastic optical networks," IEEE J. on Sel. Areas Commun. 31, 4–12 (2013).
- J. Zhang, Y. Zhao, X. Yu, J. Zhang, M. Song, Y. Ji, and B. Mukherjee, "Energy-efficient traffic grooming in sliceable-transponder-equipped IP-over-elastic optical networks [invited]," J. Opt. Commun. Netw. 7, A142–A152 (2015).
- M. Jinno, H. Takara, B. Kozicki, Y. Tsukishima, Y. Sone, and S. Matsuoka, "Spectrum-efficient and scalable elastic optical path network: architecture, benefits, and enabling technologies," IEEE Commun. Mag. 47, 66–73 (2009).
- O. Gerstel, M. Jinno, A. Lord, and S. B. Yoo, "Elastic optical networking: a new dawn for the optical layer?" IEEE Commun. Mag. 50, s12–s20 (2012).
- B. C. Chatterjee, N. Sarma, and E. Oki, "Routing and spectrum allocation in elastic optical networks: A tutorial," IEEE Commun. Surv. & Tutorials 17, 1776–1800 (2015).
- Z. Zhu, W. Lu, L. Zhang, and N. Ansari, "Dynamic service provisioning in elastic optical networks with hybrid single-/multi-path routing," J. Light. Technol. 31, 15–22 (2013).

- S. K. Singh and A. Jukan, "Efficient spectrum defragmentation with holding-time awareness in elastic optical networks," J. Opt. Commun. Netw. 9, B78–B89 (2017).
- S. Fernández, I. de Miguel, R. J. Durán, J. J. Castro, N. Merayo, J. C. Aguado, L. Ruiz, P. Fernández, R. M. Lorenzo, and E. J. Abril, "Techno-economic comparison of dynamic traffic grooming strategies for elastic optical networks," in <u>2017 19th International Conference on Transparent Optical Networks (ICTON)</u>, (2017), pp. 1–4.
- M. Hadi and M. R. Pakravan, "Energy-efficient fast configuration of flexible transponders and grooming switches in ofdm-based elastic optical networks," J. Opt. Commun. Netw. 10, 90–103 (2018).
- A. Ferrari, A. Napoli, J. K. Fischer, N. Costa, A. D'Amico, J. Pedro, W. Forysiak, E. Pincemin, A. Lord, A. Stavdas et al., "Assessment on the achievable throughput of multi-band ITU-T G. 652. D fiber transmission systems," J. Light. Technol. 38, 4279–4291 (2020).
- M. Cantono, R. Schmogrow, M. Newland, V. Vusirikala, and T. Hofmeister, "Opportunities and challenges of c+l transmission systems," J. Light. Technol. 38, 1050–1060 (2020).
- R. K. Jana, B. C. Chatterjee, A. P. Singh, A. Srivastava, B. Mukherjee, A. Lord, and A. Mitra, "Quality-aware resource provisioning for multiband elastic optical networks: a deep-learning-assisted approach," J. Opt. Commun. Netw. 14, 882–893 (2022).
- E. Etezadi, F. Arpanaei, C. Natalino, E. Agrell, L. Wosinska, P. Monti,
   D. Larrabeiti, and M. Furdek, "Joint fragmentation- and qot-aware rbmsa in dynamic multi-band elastic optical networks," in <u>2024 24th International Conference on Transparent Optical Networks (ICTON)</u>, (2024), pp. 1–5.
- M. S. Ghasrizadeh, F. Arpanaei, and H. Beyranvand, "Qot-aware tree selection, routing, modulation, and spectrum assignment for filterless eons over the C+L -band," J. Opt. Commun. Netw. 16, 127–141 (2024).
- M. Mehrabi, H. Beyranvand, M. J. Emadi, and F. Arpanaei, "Efficient statistical QoT-aware resource allocation in EONs over the C+L-band: a multi-period and low-margin perspective," J. Opt. Commun. Netw. 16, 577–592 (2024).
- F. Arpanaei et al., "Synergizing hyper-accelerated power optimization and wavelength-dependent QoT-aware cross-layer design in next-generation multi-band eons," IEEE J. on Sel. Areas Commun. 43, 1840–1855 (2025).
- F. Arpanaei, J. M. Rivas-Moscoso, I. De Francesca, J. A. Hernandez, A. Sanchez-Macian, M. R. Zefreh, D. Larrabeiti, and J. P. Fernandez-Palacios, "Enabling seamless migration of optical metro-urban networks to the multi-band: unveiling a cutting-edge 6D planning tool for the 6G era," J. Opt. Commun. Netw. 16, 463–480 (2024).
- M. N. Dharmaweera, R. Parthiban, and Y. A. Şekercioğlu, "Toward a power-efficient backbone network: The state of research," IEEE Commun. Surv. & Tutorials 17, 198–227 (2015).
- G. Zhang, M. De Leenheer, and B. Mukherjee, "Optical traffic grooming in ofdm-based elastic optical networks [invited]," J. Opt. Commun. Netw. 4, B17–B25 (2012).
- J. Leuthold, R. Bonk, P. Vorreau, S. Sygletos, D. Hillerkuss, W. Freude, G. Zarris, D. Simeonidou, C. Kouloumentas, M. Spyropoulou, I. Tomkos, F. Parmigiani, P. Petropoulos, D. Richardson, R. Weerasuriya, S. Ibrahim, A. Ellis, C. Meuer, D. Bimberg, R. Morais, P. Monteiro, S. Ben Ezra, and S. Tsadka, "An all-optical grooming switch with regenerative capabilities," in 2009 11th International Conference on Transparent Optical Networks, (2009), pp. 1–4.
- J. Zhang, Y. Ji, M. Song, Y. Zhao, X. Yu, J. Zhang, and B. Mukherjee, "Dynamic traffic grooming in sliceable bandwidth-variable transponderenabled elastic optical networks," J. Light. Technol. 33, 183–191 (2015).
- D. M. Manias, J. Naoum-Sawaya, A. Shami, A. Javadtalab, M. Hemmati, and Y. You, "Robust traffic grooming and infrastructure placement in OTN-over-dwdm networks," J. Opt. Commun. Netw. 15, 553–568 (2023).
- M. N. Dharmaweera, J. Zhao, L. Yan, M. Karlsson, and E. Agrell, "Traffic-grooming- and multipath-routing-enabled impairment-aware elastic optical networks," J. Opt. Commun. Netw. 8, 58–70 (2016).
- P. Poggiolini and M. Ranjbar-Zefreh, "Closed form expressions of the nonlinear interference for UWB systems," in 2022 European

- Conference on Optical Communication (ECOC), (2022), pp. 1-4.
- M. R. Zefreh and P. Poggiolini, "A GN-model closed-form formula supporting ultra-low fiber loss and short fiber spans," ArXiv. Accessed June 20, 2023. /abs/2111.04584. (2021).
- Y. Jiang, A. Nespola, A. Tanzi, S. Piciaccia, M. R. Zefreh, F. Forghieri, and P. Poggiolini, "Experimental test of a UWB closed-form EGN model," in 49th European Conference on Optical Communications (ECOC 2023), (2023).
- P. Poggiolini, G. Bosco, A. Carena, V. Curri, Y. Jiang, and F. Forghieri, "The GN-model of fiber non-linear propagation and its applications," J. Light. Technol. 32, 694–721 (2014).
- A. Alvarado, D. J. Ives, S. J. Savory, and P. Bayvel, "On the impact of optimal modulation and fec overhead on future optical networks," J. Light. Technol. 34, 2339–2352 (2016).
- F. Arpanaei et al., "A comparative study on routing selection algorithms for dynamic planning of EONs over C+L bands," in <u>Advanced Photonics</u> <u>Congress 2023</u>, (Optica Publishing Group, 2023), p. NeM3B.4.
- Y. Teng, C. Natalino, F. Arpanaei, H. Li, A. Sánchez-Macián, P. Monti, S. Yan, and D. Simeonidou, "DRL-assisted QoT-aware service provisioning in multi-band elastic optical networks," J. Light. Technol. pp. 1–13 (2025).
- 32. R. Jain, <u>The Art of Computer Systems Performance Analysis:</u>
  <u>Techniques for Experimental Design, Measurement, Simulation, and Modeling (John Wiley & Sons, 1991).</u>
- F. Arpanaei et al., "A digital twin-driven framework for cost-effective upgrading from C-band to multi-band optical networks," in 2025
   25th Anniversary International Conference on Transparent Optical Networks (ICTON), (2025), pp. 1–4.